Effect of Acid Etching Time in Ti_3C_2 MXene's Interlayer Spacing and Conductivity

Shanna Marie M. Alonzo, Rabin Dahal, Moses D. Ashie, and Bishnu Prasad Bastakoti[1*]

[1] Department of Chemistry, North Carolina Agricultural and Technical State University, Greensboro, NC, United States
Corresponding author: bpbastakoti@ncat.edu

Materials with sheet-like morphologies often form interconnected networks of layers or flakes, offering continuous channels for electron and ion transport in electrochemical energy storage applications [1],[2]. One such material is the recently discovered class of 2-D transition metal carbides/nitrides, called MXene, whose general formula is $M_{n+1}X_nT_x$ (where M = transition metal; n = 1, 2, or 3; X = carbon or nitrogen; and T_x = termination group such as –F, –OH, and/or =O) [3],[4]. Ti_3C_2, one of the most studied MXene, can be synthesized by selectively etching the aluminum layer in Ti_3AlC_2 (also called MAX phase) [5]. The most straightforward technique to exfoliate this layer is by wet-chemical etching with high-concentration hydrofluoric acid (HF) [6],[7]. In this work, the effect of etching time on the morphology, interlayer spacing, and electrical conductivity of the resultant MXene was studied.

After adding 50% HF to the MAX phase precursor, a displacement process occurred wherein the aluminum layer was exfoliated to form aluminum fluoride (AlF_3) [6]. Hydrogen gas was also generated, which appeared as aggressive bubbling during synthesis [8]. The resulting Ti_3C_2 would further react with HF and H_2O, forming fluorinated and hydroxylated MXene layers, i.e. $Ti_3C_2F_2$ and $Ti_3C_2(OH)_2$ [8]. After etching at room temperature at various durations (2 hours, 5 hours, and 3 days), the characteristic x-ray diffraction (XRD) peak of Ti_3AlC_2 at $2\theta \approx 39^o$ vanished (**Fig. 1 a**), verifying the significant removal of the MAX phase's Al-layer [9]. This confirms the crystal structure of Ti_3AlC_2 has indeed changed to Ti_3C_2 MXene. The diffraction peak at $2\theta \approx 9.3^o$ which corresponds to the (002) plane shifted to lower angles, indicating an increase in the interlayer spacing of the nanolayers [1]. Using Bragg's law, the d-spacing values for MAX, MXe-2h, MXe-5h, and MXe-3d were found to be 9.46 Å, 10.12 Å, 10.27 Å, and 10.84 Å, respectively. These equated to c-lattice parameters ($c = 2d_{(002)}$) of 18.92 Å, 20.24 Å, 20.55 Å, and 21.68 Å, respectively. When compared to the pristine MAX phase, MXe-3d showed the highest increase (14.57%) in the c-lattice parameter. MXe-2h and MXe-5h increased by 6.97% and 8.59%, respectively. Moreover, only the MXe-3d displayed the characteristic peak of the (008) plane at $2\theta \approx 27.5^o$, and as demonstrated by the peak intensities, it also had the highest crystallinity [10]. X-ray photoelectron spectroscopy (XPS) further confirmed the introduction of –F and –OH termination groups after etching. The XPS survey scan spectra showed that MXe-2h, MXe-5h, and MXe-3d were mainly composed of Ti, C, O, and F [11],[12].

The scanning electron microscopy (SEM) image of Ti_3AlC_2 (**Fig. 1b**) displayed the typical ternary layered structure of the MAX phase [10]. While MXe-2h (**Fig. 1c**) showed little change in morphology, MXe-5h (**Fig. 1d**) and MXe-3d (**Fig. 1e**) showed significant changes. The last two were clearly exfoliated, exhibiting accordion-like stacked layers. The SEM–energy dispersive x-ray (EDX) analysis showed a decreasing trend in the atomic weight percent of aluminum as the etching duration increased (MAX = 9.9%; MXe-2h = 8.5%; MXe-5h = 2.1%; MXe-3d = 1.9%).

The samples were then employed as active materials for electrochemical tests to evaluate their suitability as supercapacitors. The active material, polyvinylidene fluoride (binder), and conductive carbon black were combined in an 80:10:10 mass ratio to construct the working electrode. N-methyl-2-pyrrolidone was used as the solvent, and pre-treated carbon cloth measuring 1.5 cm x 1.0 cm was used as the current collector. The prepared working electrodes were dried in a vacuum oven at 60ºC for 14 h. The

specific capacitance (F/g) was calculated from cyclic voltammetry (CV) using the formula $C_s = \frac{\int_{V_1}^{V_2} Idv}{2sm\Delta V}$ where C_s is the specific capacitance (F/g), $\int_{V_1}^{V_2} Idv$ is the integral CV curve area (AV), s is the scan rate (V/s), m is the mass of the active material (g), and ΔV is the potential window [13]. The results showed significant improvement in the specific capacitance when the aluminum layer was etched out from the MAX phase. This is due to (1) the transition metal carbide is exposed when aluminum is removed, improving MXene's metallic conductivity [14]; and (2) during the charge/discharge cycle, the oxygen-terminated surface bonds and de-bonds with the hydronium ion in the H_2SO_4 electrolyte, producing pseudocapacitance [15]. Over a range of scan rates, MXe-2h consistently displayed the highest capacitance, whereas MXe-5h and MXe-3d did not significantly differ from one another. This is consistent with the well-known fact that MXene has good in-sheet conductivity and poor conductivity between sheets [16]. Given that MXe-5h and MXe-3d exhibited greater sheet separation, it makes plausible that their conductivity was somewhat lower than that of MXe-2h. The tunable interlayer spacing opens up to further exploration to design MXene-based composites. Utilizing the layer-to-layer gap allows for the insertion of other spacers, such as metal oxides, carbon nanotubes, and polymers, as well as cationic intercalation [17]. This could further improve ion transport kinetics for electrochemical energy storage uses.

In summary, Ti_3AlC_2 (MAX phase) was successfully transformed to Ti_3C_2 (MXene) by directly etching the aluminum layer with hydrofluoric acid. The reaction time dictated the interlayer spacing of the Mxene layers which in turn affected its conductivity.

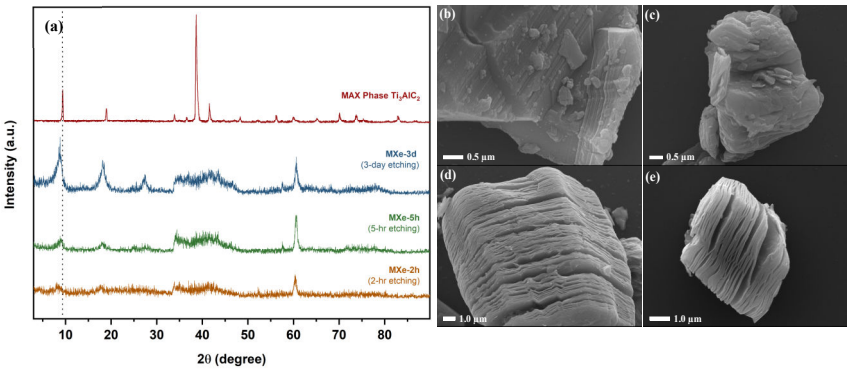

Fig. 1. (a) X-ray diffraction patterns of the as-received Ti_3AlC_2 (MAX phase) and synthesized Ti_3C_2 MXene etched at different times. Scanning electron microscopy (SEM) images of (b) Ti_3AlC_2 MAX phase and Ti_3C_2 MXene etched for: (c) 2 hours (MXe-2h), (d) 5 hours (MXe-5h), and (e) 3 days (MXe-3d).

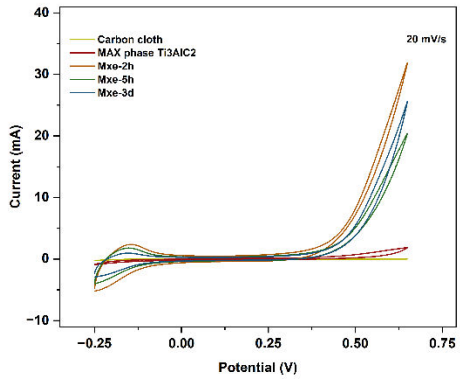

Fig. 2. Cyclic voltammetry curves in 1M H_2SO_4 electrolyte at a potential window of -0.25 V to 0.65 V, with platinum wire as the counter electrode and Ag/AgCl as reference electrode.

Acknowledgement

This work was supported by DOE BES-RENEW award number DE-SC0024611.

References

1. Y. Sun et al*., J. Memb. Sci*., vol. 591 (2019). 10.1016/j.memsci.2019.117350.
2. X. Zhu et al., *Sustain. Energy Fuels*, vol. 4 (2020), pp. 3566–3573. 10.1039/d0se00448k.
3. A. Feng et al., *Mater. Des*., vol. 114 (2017), pp. 161–166. 10.1016/j.matdes.2016.10.053.
4. S. H. Overbury et al., *J. Am. Chem. Soc*., vol. 140 (2018), pp. 10305–10314. 10.1021/jacs.8b05913.
5. Y. Gogotsi and Q. Huang, *ACS Nano*, vol. 15 (2021), pp. 5775–5780. 10.1021/acsnano.1c03161.
6. U. Rahman et al., *Molecules* vol. 27 (2022), p. 4909. https://doi.org/10.3390/molecules27154909
7. A. Thakur et al., *Small Methods* vol. 7 (2023), pp. 1–16. 10.1002/smtd.202300030.
8. M. Naguib et al., *Adv. Mater*. vol. 23, (2011), pp. 4248–4253. 10.1002/adma.201102306.
9. A.C. Khot et al., *ACS Appl. Mater. Interfaces* vol. 13 (2021), pp. 5216–5227. 10.1021/acsami.0c19028.
10. K. Chen et al., *Res. Chem. Intermed*. vol. 48 (2022), pp.4443–4458. 10.1007/s11164-022-04830-6.
11. J. Cao et al., *RSC Adv*. vol. 9 (2019), pp. 34152–34157. 10.1039/c9ra06091j.
12. L. Yao et al., *J. Mater. Sci. Mater. Electron*. vol. 32 (2021), pp. 27837–27848. 10.1007/s10854-021-07166-w.
13. M. Naguib et al., *Adv. Mater*., vol. 26 (2014), pp. 992–1005. 10.1002/adma.201304138.
14. C. Zhan et al., *J. Phys. Chem. Lett*. vol. 9 (2018), pp. 1223–1228. 10.1021/acs.jpclett.8b00200.
15. M.S. Cao et al., *Chem. Eng. J*., vol. 359 (2019), pp. 1265–1302. 10.1016/j.cej.2018.11.051.
16. A. Mateen et al., *J. Energy Storage* vol. 71 (2023). 10.1016/j.est.2023.108151.
17. S.M.M. Alonzo et al., *Sci. Rep*. vol. 13 (2023). 10.1038/s41598-023-48958-w.